J Solid State Electrochem (2014) 18:2955–2961
DOI 10.1007/s10008-014-2528-6

ORIGINAL PAPER

Microvials with tungsten nanowire arrays

Stefanie Drensler · Srdjan Milenkovic · Achim Walter Hassel

Received: 21 March 2014 / Accepted: 28 May 2014 / Published online: 11 July 2014

Abstract Nanostructured eutectic NiAl–W, fabricated using a Bridgman-type directional solidification facility, combines the advantages of single individual nanowires with the benefit of a conductive macroscopic matrix. Through an electrochemical dissolution step, using conditions derived from the combined Pourbaix diagrams of all three elements involved, the NiAl matrix is selectively dissolved allowing the release of embedded W nanowires. An application of micro-scale electrochemical techniques, such as scanning droplet cell microscopy, facilitates not only selective but moreover local matrix dissolution. Such a local dissolution leads to the formation of cavities on the micro-scale containing arrays of single crystalline W nanowires. In this connection, the depth and volume of fabricated microvials can directly be determined from the charge consumed during potentiostatic dissolution. A subsequent surface functionalisation enhances the hydrophobic behaviour, which is already observed for non-functionalised nanowire arrays, resulting in measured contact angles close to the border to superhydrophobicity.

Keywords NiAl–W · Eutectic alloy · Tungsten nanowires · Selective dissolution · Scanning droplet cell microscopy

S. Drensler · A. W. Hassel
Institute for Chemical Technology of Inorganic Materials, Johannes Kepler University Linz, Altenberger Str. 69, 4040 Linz, Austria

S. Milenkovic
IMDEA Materials Institute, Eric Kandel 2, Tecnogetafe, 28906 Getafe, Spain

A. W. Hassel (✉)
Christian Doppler Laboratory for Combinatorial Oxide Chemistry, Institute for Chemical Technology of Inorganic Materials, Johannes Kepler University Linz, Altenberger Str. 69, 4040 Linz, Austria
e-mail: achimwalter.hassel@jku.at

Introduction

The fast developing field of micro- and nanoscale devices requires scaling down not only the dimensions of the materials used, but also the electrochemical techniques utilised for both, manipulation and characterisation. Throughout the past decade, synthesis and application of nanowires became a major topic of research. Semiconducting nanowires like InP, InAs and GaAs [1], but also oxides [2–4] and even metal nanowires have been manufactured. Metallic nanowires, like Ni [5, 6] or Au [7], are usually fabricated using template assisted electrodeposition methods. Chemical deposition of Pt [8] and wet-chemical preparation routes as in the case of Au [9] nanowires have also been implemented.

Out of the vast amount of available materials, refractory metal nanowires — like Re, Mo or W — gained significant interest due to their unique combination of mechanical and chemical material properties [10–12].

For manufacturing W nanowires, in particular, a large variety of vapour deposition techniques have been developed [13–16].

However, subsequent handling and manipulation of the produced nanowires remains a challenging task. An organisation of nanowires in arrays combined with a conductive surrounding substrate simplifies not only the handling, but also the further use of the fabricated nanowires. Directional solidification under usage of a Bridgman type crystal growth facility allows fabricating such nanostructured alloys, resulting in arrays of single crystalline nanowires embedded in a matrix material. During the eutectic growth process, the size and distribution of the embedded nanowires can directly be controlled through the process parameters. This technique has already been successfully applied to fabricate Au nanobelts from eutectoid FeAu [17], Cu nanowires from eutectic AgCu [18] and for the production of refractory metal

nanowires from pseudobinary eutectic NiAl–*X* (*X*=Re, Mo, W) [19].

The further use of the nanowires requires a chemical or electrochemical release from its surrounding matrix material. Therefore adequate conditions have to be chosen allowing a selective and simultaneous dissolution of both Ni and Al, whereas W remains intact. The complete selective dissolution of directionally solidified NiAl–W (ds-NiAl-W) allows a large-scale synthesis of up to gram amounts of W nanowires [20].

Besides this, a partial release is also possible, revealing nanowires possessing a tuneable length. If the area of interest is further decreased to sub-millimeter scale, alternative techniques for both localized and selective electrochemical dissolution have to be found. For that particular purpose, scanning droplet cell microscopy (SDCM) [21–24] is a powerful tool that can perform all types of electrochemical methods, allowing users to address reproducibly small areas of the sample.

In this work, microvials containing nanowire arrays are fabricated through selective dissolution of directionally solidified NiAl–W using SDCM. The depth of the fabricated vials can directly be derived from obtained transients additionally allowing determination of the length of the exposed nanowires. Subsequent surface functionalisation of the W nanowires is pointing at possible applications of the manufactured microvials.

Experimental

Sample preparation

NiAl–W pre-alloys were prepared through induction melting and drop casting from metal powders of Ni (99.97 wt.%) and Al (99.99 wt.%) in equiatomic ratio under addition of 1.5 at.% of W (99.9 wt.%), representing the composition at the eutectic point of the system. In a next step the alloy was then directionally solidified using a Bridgman furnace. Therefore, the samples were cut into cylindrical shape and placed inside an alumina crucible. The samples were heated to a temperature of 1,700 °C to ensure uniform melting. Subsequent directional solidification was performed with a pulling rate of 200 mm h^{-1} under a thermal gradient of 40 K cm^{-1}.

Afterwards the samples were cut — perpendicular or in parallel to the growth direction of contained nanowires — into discs with an initial thickness of 2 mm. The samples were further thinned by a mechanical grinding process until a final thickness of 350 μm. Surface finishing was performed through diamond polishing up to a final grade of 3 μm. After cleaning with ethanol and deionised water, the sample was fixed to a stainless steel plate using silver paste to ensure proper electrical contact.

Selective dissolution

Figure 1 shows a superposition of the Pourbaix diagrams [25] of the three elements (Ni, Al and W) present in the eutectic. Assuming that the initial concentration of the dissolved species in solution is $\leq 10^{-6}$ M, a simultaneous dissolution of the matrix materials — Ni and Al — becomes feasible at pH values lower than 4 and potentials starting from −400 mV versus standard hydrogen electrode (SHE). Within the electrochemical window — in this certain pH range — tungsten passivates, protecting the embedded nanowires from dissolution. Hence, the chosen conditions for the selective matrix dissolution were a potential of 250 mV (SHE) and a 1 M HCl with a pH slightly below 0.

Localized, electrochemical dissolution in the sub-millimeter range can be performed using SDCM.

A borosilicate glass capillary with an outer diameter of 2.5 mm (Hilgenberg GmbH, Malsfeld, Germany) was tapered using a capillary puller (Narishige, Tokyo, Japan) and subsequently ground with an in-house built micro grinder up to 2400 grid SiC emery paper. The capillary was then cleaned using ethanol and deionised water and dried using nitrogen. An additional silicone gasket at the tip of the capillary was produced through dipping the capillary into liquid silicone (Momentum, Albany, USA) and subsequent drying by flushing with nitrogen. The capillary was then mounted into a polypropylene screw equipped with an o-ring to avoid electrolyte leakage.

A miniaturized silver/silver chloride reference electrode (μ-RE) was prepared through electrochemical deposition of AgCl onto a silver wire with a diameter of 100 μm. The coated silver wire was then placed inside a small glass capillary (Hilgenberg GmbH). Then the pre-heated capillary was filled with a 3 M KCl solution containing 4 wt.% agar. The upper part of the capillary was sealed using epoxy resin to avoid

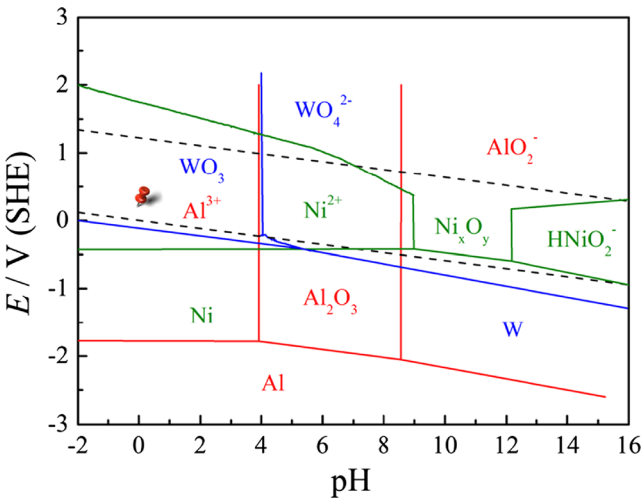

Fig. 1 Superposition of the Pourbaix diagrams of Ni, Al and W considering lines for an initial concentration of the dissolved species of 10^{-6} M. The *red pin* indicates the conditions for a simultaneous dissolution of the matrix elements Ni and Al under concurrent oxidation of W

water evaporation from the gelled electrolyte. A detailed description of the preparation process for the manufactured reference electrodes can be found elsewhere [26].

The counter electrode (CE) consists of a gold wire with a thickness of 100 μm (99.999 %; Wieland Dentaltechnik, Pforzheim, Germany) which was wrapped around the before prepared μ-RE. Both electrodes were fixed inside a second screw using epoxy resin. The screws containing the set of electrodes and the glass capillary were fixed to an acrylic block equipped with an additional opening functioning as the electrolyte inlet, as shown in Fig. 2.

Electrochemical dissolution was performed using a potentiostat (Ivium Technologies, Eindhoven, the Netherlands) with SDCM working in contact mode under variation of the dissolution time. This mode was in particular chosen on one hand to precisely determine the diameter of produced microvials. On the other hand, an operation in contact mode is necessary to prevent electrolyte leakage caused by hydrogen gas evolution at the CE. The SDCM cell was automatically positioned using a gantry robot built from three linear stages [27].

Analytical methods

Characterisation concerning microstructure and surface analysis was done using scanning electron microscopy (SEM) (Zeiss LEO 1540 XB). The depth profile of fabricated microvials was measured using a DekTak XT stylus profilometer (Bruker Corporation, USA).

Silanisation

For a study on surface functionalisation, ds-NiAlW samples were cut into discs with 2-mm thickness. The samples were ground and diamond polished up to 3 μm. After cleaning with ethanol, and deionised water in an ultrasonic bath, the samples were dried with nitrogen. A series of samples was chemically etched in a mixture of $HCl/H_2O_2/H_2O$ (1:1:8) under variation of the etching time from 0 to 15 min. Subsequently the samples were immersed in a solution of 0.2 % of *n*-octadecyltrichlorosilane (OTS) in toluene for a duration of 2 h for silanisation. After washing with toluene, isopropanol and deionised water, the samples were dried in nitrogen flow and the contact angle was measured using a contact angle system (DataPhysics, Filderstadt, Germany). The contact angle was determined using droplets of deionised water (2 μl) under utilisation of the circle fitting model.

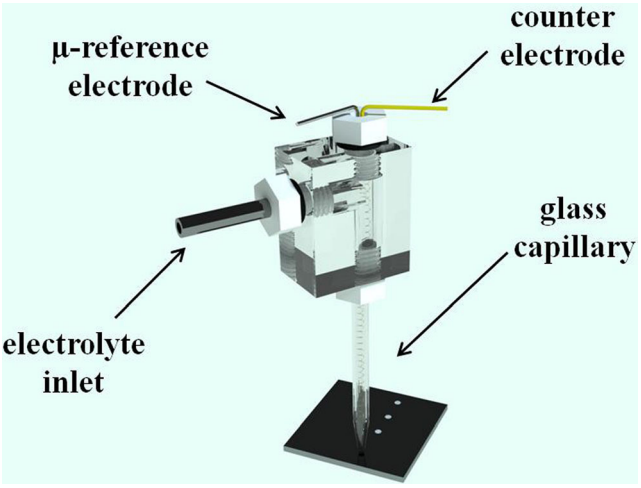

Fig. 2 Schematic drawing of the SDCM setup used for selective dissolution of the NiAl matrix

Results and discussion

Directional solidification is an effective and template-free technique for the production of refractory metal nanowires. The microstructure of manufactured ds-NiAlW is a complex result of the chosen processing conditions of the solidification process. Two main parameters, the thermal gradient and the pulling speed, determine both the size but also the spacing of produced W nanowires. As shown in an earlier study, the diameter of the nanowires is decreasing with increasing pulling rate, reaching a minimum diameter at the highest feasible rate of the equipment used (200 mm h^{-1}) [28]. Such a high growth rate not only minimizes the wire diameter but also leads to the formation of a cellular microstructure with nanowires emerging from the centre of such a cell, radially growing towards the eutectic cell boundary. Hence, high pulling rates lead to a maximized overall surface area of contained tungsten nanowires.

Since the produced nanowires are surrounded by a matrix material, Ni and Al in equiatomic ratio, a dissolution step is required to release the embedded nanowires. Matrix dissolution is feasible by both chemical etching using a mixture of H_2O_2, HCl and H_2O as shown by Hassel et al. [29] or by electrochemical matrix dissolution [20]. Electrochemical dissolution has the advantage of a precise control upon the length of the exposed wires but also on the amount of dissolved matrix material. The superposition of the Pourbaix diagrams shows that at the chosen potential of 250 mV (SHE), both Ni and Al are dissolving while W is oxidized, leading to the formation of WO_3 at the nanowire surface. Here, the usage of SDCM technique not only enables a selective dissolution but furthermore allows a local matrix removal. As shown in Fig. 3, selective dissolution results in the formation of microvials, i.e., cavities with nanowires protruding from their bottom. An automated positioning system allows determining the distance in between two microvials offering a precise tool to control the spatial distribution. The diameter of produced microvials is thereby directly coupled to the diameter of the used capillary. As illustrated in Fig. 3b, showing microvials created after potentiostatic dissolution for 5 or 15 min, the

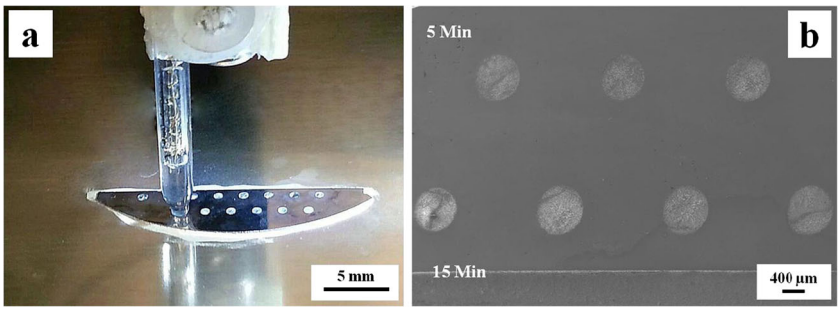

Fig. 3 Usage of SDCM allows both a selective and local dissolution of the NiAl matrix under precise control of the spatial resolution (**a**). The variation of the dissolution time enables the production of microvial arrays with W nanowires maintaining a highly reproducible spot size (**b**)

operation in confined droplet mode leads to a high reproducibility of the addressed area.

The fact that the microstructure and hereby the orientation of the nanowires is already fixed through the solidification parameters, allows to choose the orientation of exposed nanowires by cutting the sample either perpendicular or in parallel to the growth direction. Typical microstructures of such samples can be found in Fig. 4.

Since a precise determination of the overall volume of the produced microvials and their corresponding depth is difficult due to nanowires present in the formed cavities, an alternative approach to conventional depth profiling methods has to be found.

The volume of a theoretical microvial is mainly consisting of the volume of the matrix material, holding with 98.5 at.% the majority on the overall vial volume, plus the volume of the minor phase, the contained nanowires. Therefore the vial volume can be expressed by the following equation:

$$V_{\text{vial}} = V_{\text{matrix}} + V_{\text{nanowires}} \tag{1}$$

As the charge Q, consumed during potentiostatic matrix dissolution, is directly proportional to the amount of the dissolved matrix material, an integration of the recorded current over time in between t_{start} and t_{end} can be used to approximate the dissolved mass.

Hence, the volume of a formed cavity can be calculated based on the overall charge consumed. Assuming a stoichiometric current efficiency of the dissolution process and simultaneous dissolution of both Ni and Al, the mass m of the dissolved matrix can be calculated using Faraday's law:

$$m = \frac{Q \cdot M_{\text{NiAl}}}{z \cdot F}, \tag{2}$$

where M_{NiAl} is the sum of the molar mass of Ni and Al (85.67 g mol^{-1}), z is the sum valence number of transferred ions, F is the Faraday constant (96485.34 C mol^{-1} C mol^{-1}), and the charge Q of 175.5 mC for 300 s and 57.5 mC for 100 s dissolution, calculated from the chronoamperometric measurements.

With the density of pure NiAl of 5.94 g cm^{-3} [30], a volume of V_{matrix}=5.25 nl was calculated for a typical measuring spot with a dissolution time of 300 s and a volume of 1.72 nl for a duration of 100 s.

Assuming that the formed vials have the typical shape of a spherical cap, the volume V_{sc} can be calculated using the following equation:

$$V_{\text{sc}} = \frac{h^2 \cdot \pi}{3}(3r - h), \tag{3}$$

where h is the depth of the microvial and r is the radius of the full sphere. The variable r is related to the measured radius of

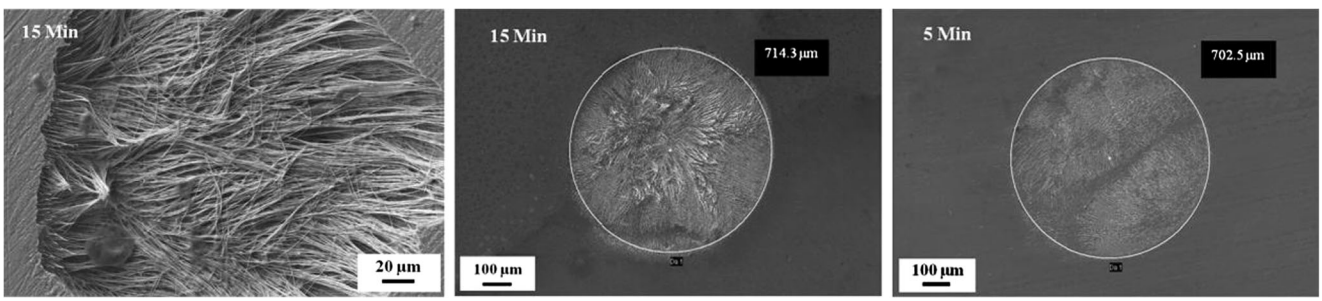

Fig. 4 Microvials with W-nanowire arrays after selective matrix dissolution of samples cut parallel to the growth direction (*left*) and perpendicular to the growth direction

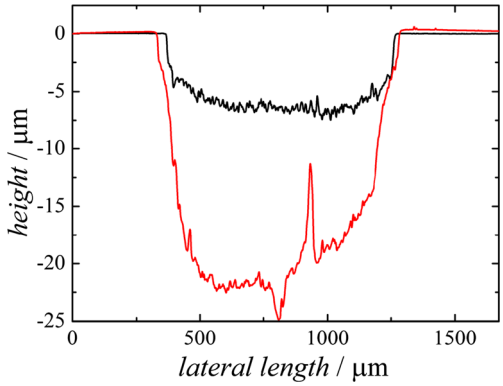

Fig. 5 Depth profiles of two typical microvials for a dissolution time of 100 s (*black line*) and 300 s (*red line*) obtained by profilometry

the microvials a, obtained by SEM, through the following expression:

$$r = \frac{a^2 + h^2}{2h} \tag{4}$$

Replacing r in Eq. 3 by the expression given above, and rearranging the equation for h results in a calculated depth of 30.92 µm for 300 s dissolution and a depth of 10.22 µm for a matrix dissolution of 100 s.

Figure 5 shows the depth profiles of two microvials obtained for dissolution times of 100 and 300 s determined by profilometer measurements. The measured minima show a depth of 24.82 µm for a dissolution time of 300 s and a depth of 7.47 µm for the respective spot with 100 s dissolution.

After an initial decrease, which is characteristic for an electrochemical dissolution using SDCM in confined droplet mode allowing the production of sharp edged structures, the slow decrease in height is already indicating the spherical form of the created vial. When reaching the bottom of the pit the measured oscillations show an increased roughness caused by nanowires emerging from the bottom of the vial. Hence, a determination of the depth is difficult. Nevertheless, an upper-limit estimation can be made by choosing the local minima observed in these measurements.

The height differences between calculated and measured values are a result of several factors. First, measured minima were taken as reference values for comparison, although these minima depend on the actual spot on the sample chosen for dissolution. As the eutectic shows a characteristic cellular structure at these high pulling rates, a minimum can easily be found at the boundary between two neighbouring eutectic cells but is rather unlikely to be found if the vial is located centred in the origin of a formed eutectic cell. The latter is based on the fact, that W nanowires show both a high elasticity and ductility as shown by Cimalla et al. [10], who performed mechanical tests on single W nanowires. During profilometry, the elasticity of these wires together with the relatively large tip size of the profilometer used (2 µm) can lead to the sharp peaks appearing at the bottom of the vial, visible in Fig. 5, probably originating from the elastic deformation of embedded nanowires.

The adaptable capillary diameter in SDCM, used together with a gantry robot positioning system, allows producing arrays of microvials, not only with a distinct distance, vial

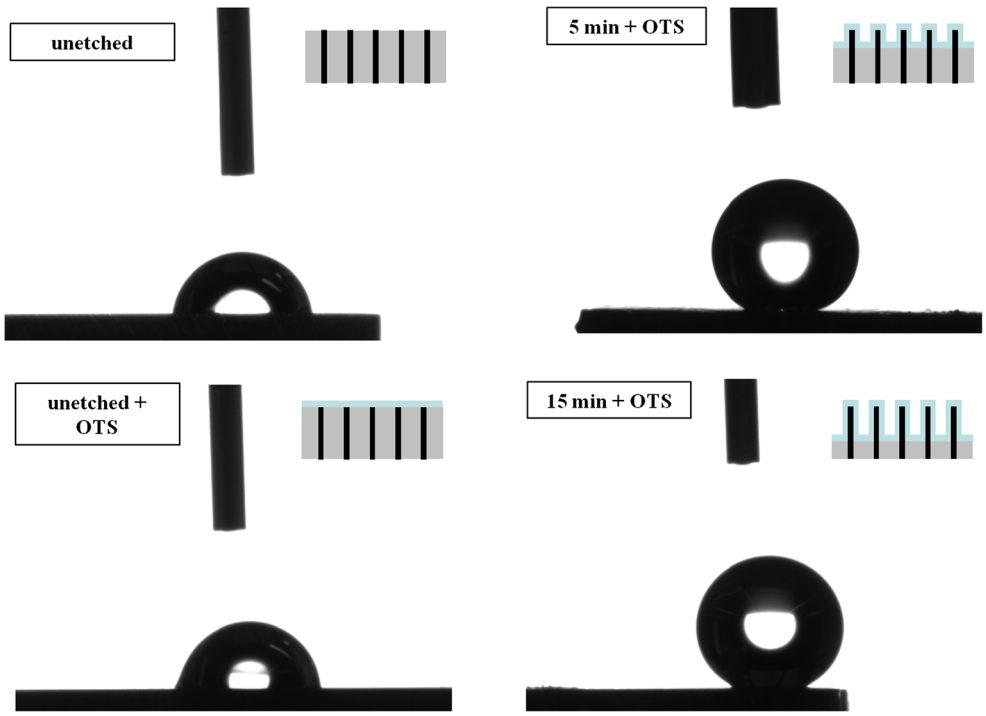

Fig. 6 Contact angle measurement for unetched ds-NiAl–W samples (*left*) and for chemically etched samples for the indicated time (*right*) functionalised using OTS

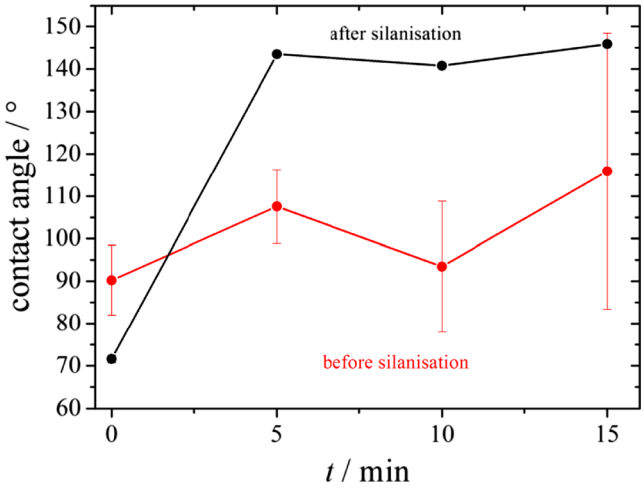

Fig. 7 Measured contact angles before and after surface functionalisation using OTS as a function of the etching time. Silanisation leads to increased contact angle of etched samples and minimizes the measured error

diameter and depth but also with nanowires possessing a tuneable exposure length. This high structural versatility, already points at the large variety of potential applications.

The pH sensitivity of tungsten oxide was already discovered in the beginning of the last century by Baylis [31]. Due to the conditions chosen for matrix dissolution, tungsten is oxidised leading to a coverage of the nanowires with an approx. 6 nm thick oxide layer on the nanowire surface [19]. As shown in a recent study, not only single [32] but furthermore arrays of nanowires protruding from a created microvial can be used for pH sensing [33]. Here, the usage of either SDCM filled with the test solution or a measurement in single droplets placed in a microvial minimizes the amount of test solution needed.

Also a subsequent surface functionalisation of W nanowires is possible. Coating of etched NiAl–W samples with 0.2 % OTS dissolved in toluene, leads to a silanised surface showing a change from hydrophilic to hydrophobic behaviour. In this particular case, chemical matrix dissolution was chosen as only one side of the disc shaped sample should be etched. This enables to measure several spots per sample to minimize the influence of the irregular, cellular structure onto the contact angles measured. As illustrated in Fig. 6, both bare unetched and unetched, silanised surfaces show a hydrophilic behaviour. When the nanowires are released from the NiAl matrix the contact angle just slightly increases, however a high local dependency of the contact angle was found for all non-functionalised samples resulting in large values for the standard deviation.

Figure 7 shows the drastic increase of the contact angle when etched samples were treated with OTS. A maximum contact angle of 145.8±0.67° was reached for an etching time of 15 min, which is very close to the border of superhydrophobicity. Although for the different etching times no severe differences in the contact angle were found, the characteristic droplet shape formed on silanised surfaces indicates a Wenzel-like behaviour [34], which was also found for NiAl–Re sputtered with poly(tetrafluoroethylene) (PTFE) [35].

Such a hydrophobic spot surrounded by a matrix material showing a hydrophilic behaviour, could be used to locate or immobilise droplets of hydrophobic liquids like oils or long chained alcohols. Sputtering with PTFE and subsequent skimming is an alternative way of producing thin hydrophobic layers covering both the remaining matrix inside the formed microvial and contained nanowires. Therefore also the reverse is possible, where sputtering of partially masked ds-NiAl-W and subsequent matrix dissolution leads to rather hydrophilic spots surrounded by a hydrophobic PTFE-covered sample surface. A schematic drawing of these functionalised microvials can be found in Fig. 8.

Conclusions

Directional solidification of eutectic NiAl–W results in arrays of W nanowires embedded in a NiAl matrix. The usage of SDCM allows for a local electrochemical dissolution of the NiAl matrix under conditions derived from the superposition of the Pourbaix diagrams of all respective elements. The volume of a created microvial, and therefore the exposure length of contained nanowires, can directly be determined through the duration of potentiostatic dissolution. Theoretical calculations show a depth of 30.92 μm for 300 s dissolution and 10.22 μm for a matrix dissolution of 100 s. A survey of the obtained values, carried out using a stylus profilometer, showed values of 24.82 μm for a dissolution time of 300 s and a depth of 7.47 μm for the respective spot with 100 s dissolution time. A major drawback of experimental depth profiling is the large tip size, as compared to nanowires having an average diameter of around 300 nm. Additionally the fact that the W nanowires are protruding from the bottom of the formed vials, hinders a precise depth determination.

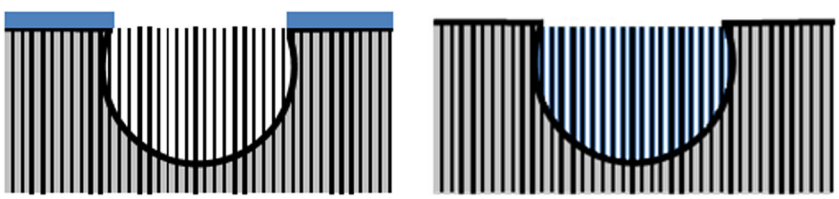

Fig. 8 Schematic drawings of functionalized microvials coated with a hydrophobic layer the sample surface (*left*) and sputtered with PTFE (*right*) under subsequent mechanical removal of the outermost surface layer

Subsequent functionalisation of released nanowires is possible by a chemical surface reaction of the oxide-covered W nanowires with an OTS solution. Chemically etched and silanised nanowire arrays show drastically increased contact angles close to those of superhydrophobicity. These observations combined with the latest developments in localised electrochemical techniques can be used to design arrays of functionalised microvials containing large amounts of high-aspect ratio nanowires.

Acknowledgments The financial support by the Austrian Federal Ministry of Economy, Family and Youth and the National Foundation for Research, Technology and Development (Christian Doppler Laboratory for Combinatoriall Oxide Chemistry - COMBOX) is gratefully acknowledged. The authors are indepted to Jan Philipp Kollender for providing the schematic drawing of the SDCM.

References

1. Banerjee S, Dan A, Chakravorty D (2002) Review synthesis of conducting nanowires. J Mater Sci 37:4261–4271
2. Yang P, Yan H, Mao S, Russo R, Johnson J, Saykally R, Morris N, Pham J, He R, Choi H-J (2002) Controlled growth of ZnO nanowires and their optical properties. Adv Funct Mater 12:323–331
3. Dai ZR, Gole JL, Stout JD, Wang ZL (2002) Tin oxide nanowires, nanoribbons, and nanotubes. J Phys Chem B 106:1274–1279
4. Daoud WA, Pang GKH (2006) Direct synthesis of nanowires with anatase and TiO_2-B structures at near ambient conditions. J Phys Chem B 110:25746–25750
5. Lin S, Chang S, Liu R, Hu S, Jan N (2004) Fabrication and magnetic properties of nickel nanowires. J Magn Magn Mater 282:28–31
6. Pirota K, Navas D, Hernández-Vélez M, Nielsch K, Vázquez M (2004) Novel magnetic materials prepared by electrodeposition techniques: arrays of nanowires and multi-layered microwires. J Alloys Compd 369:18–26
7. Kautek W, Reetz S, Pentzien S (1995) Template electrodeposition of nanowire arrays on gold foils fabricated by pulsed-laser deposition. Electrochim Acta 40:1461–1468
8. Han Y-J, Kim JM, Stucky GD (2000) Preparation of noble metal nanowires using hexagonal mesoporous silica SBA-15. Chem Mater 12:2068–2069
9. Vasilev K, Zhu T, Wilms M, Gillies G, Lieberwirth I, Mittler S, Knoll W, Kreiter M (2005) Simple, one-step synthesis of gold nanowires in aqueous solution. Langmuir 21:12399–12403
10. Cimalla V, Röhlig C-C, Pezoldt J, Niebelschütz M, Ambacher O, Brückner K, Hein M, Weber J, Milenkovic S, Smith AJ, Hassel AW (2008) Nanomechanics of single crystalline tungsten nanowires. J Nanomater 2008:638947
11. Philippe L, Peyrot I, Michler J, Hassel AW, Milenkovic S (2007) Yield stress of monocrystalline rhenium nanowires. Appl Phys Lett 91:111919
12. Philippe L, Wang Z, Peyrot I, Hassel AW, Michler J (2009) Nanomechanics of rhenium wires: elastic modulus, yield strength and strain hardening. Acta Mater 57:4032–4035
13. Liu ZQ, Mitsuishi K, Furuya K (2004) Features of self-supporting tungsten nanowire deposited with high-energy electrons. J Appl Phys 96:619–623
14. Liu ZQ, Mitsuishi K, Furuya K (2004) The growth behavior of self-standing tungsten tips fabricated by electron-beam-induced deposition using 200 keV electrons. J Appl Phys 96:3983–3986
15. Wang S, He Y, Zou J, Jiang Y, Xu J, Huang B, Liu CT, Liaw PK (2007) Synthesis of single-crystalline tungsten nanowires by nickel-catalyzed vapor-phase method at 850 °C. J Cryst Growth 306:433–436
16. Ross IM, Luxmoore IJ, Cullis AG, Orr J, Buckle PD, Jefferson JH (2006) Characterisation of tungsten nano-wires prepared by electron and ion beam induced chemical vapour deposition. J Phys Conf Ser 26:363–366
17. Milenkovic S, Schneider A, Hassel AW (2006) Gold nanostructures by directional solid-state decomposition. Gold Bull 39:185–191
18. Brittman S, Smith AJ, Milenkovic S, Hassel AW (2007) Copper nanowires and silver micropit arrays from the electrochemical treatment of a directionally solidified silver–copper eutectic. Electrochim Acta 53:324–329
19. Hassel AW, Bello-Rodriguez B, Smith AJ, Chen Y, Milenkovic S (2010) Preparation and specific properties of single crystalline metallic nanowires. Phys Status Solidi B 247:2380–2392
20. Hassel AW, Milenkovic S, Smith AJ (2010) Large scale synthesis of single crystalline tungsten nanowires with extreme aspect ratios. Phys Status Solidi A 207:858–863
21. Suter T, Böhni H (2001) Microelectrodes for corrosion studies in microsystems. Electrochim Acta 47:191–199
22. Mardare AI, Wieck AD, Hassel AW (2007) Microelectrochemical lithography: a method for direct writing of surface oxides. Electrochim Acta 52:7865–7869
23. Sakairi M, Sato F, Gotou Y, Fushimi K, Kikuchi T, Takahashi H (2008) Development of a novel microstructure fabrication method with co-axial dual capillary solution flow type droplet cells and electrochemical deposition. Electrochim Acta 54:616–622
24. Sánchez M, Gamby J, Perrot H, Rose D, Vivier V (2010) Microelectrochemistry of copper in NaCl solution: Comparison between conventional microelectrode and microelectrochemical cell. Electrochem Commun 12:1230–1232
25. Pourbaix M (1966) Atlas of electrochemical equilibria. Pergamon Press, Headington Hill, Oxford
26. Hassel AW, Fushimi K, Seo M (1999) An agar-based silver|silver chloride reference electrode for use in micro-electrochemistry. Electrochem Commun 1:180–183
27. Kollender JP, Mardare AI, Hassel AW (2013) Photoelectrochemical scanning droplet cell microscopy (PE-SDCM). ChemPhysChem 14: 560–567
28. Milenkovic S, Hassel AW (2009) Spatial features control of self-organised tungsten nanowire arrays. Phys Status Solidi A 206:455–461
29. Hassel AW, Smith AJ, Milenkovic S (2006) Nanostructures from directionally solidified NiAl–W eutectic alloys. Electrochim Acta 52: 1799–1804
30. Schäfer H (1997) Entwicklung und Eigenschaftscharakterisierung hochwarmfester Werkstoffe mit intermetallischer NiAl-Matrix. VDI-Verlag, Düsseldorf
31. Baylis JR (1923) Tungsten wire for hydrogen-ion determinations. J Ind Eng Chem 15:852–853
32. Fenster C, Smith AJ, Abts A, Milenkovic S, Hassel AW (2008) Single tungsten nanowires as pH sensitive electrodes. Electrochem Commun 10:1125–1128
33. Drensler S, Walkner S, Mardare CC, Hassel AW (2014) On the pH sensing properties of differently prepared tungsten oxide films. Phys Stat Sol A. Phys Stat Sol A 211:1340–1345
34. Roach P, Shirtcliffe NJ, Newton MI (2008) Progess in superhydrophobic surface development. Soft Matter 4:224–240
35. Hassel AW, Milenkovic S, Schürmann U, Greve H, Zaporojtchenko V, Adelung R, Faupel F (2007) Model systems with extreme aspect ratio, tunable geometry, and surface functionality for a quantitative investigation of the lotus effect. Langmuir 23:2091–2094